GROUNDWATER RADON RISK MAPPING IN ATHENS REGION, GEORGIA

Shahrokh Rouhani and Marc E. Dillion

AUTHORS: Shahrokh Rouhani, School of Civil Engineering, Georgia Institute of Technology, Atlanta, Georgia 30332; and Marc E. Dillon, Golder Associates Inc., Atlanta, Georgia 30341.
REFERENCE: Proceedings of the 1991 Georgia Water Resources Conference, held March 19 and 20, 1991 at The University of Georgia. Kathryn J. Hatcher, Editor, Institute of Natural Resources, The University of Georgia, Athens, Georgia.

Abstract: Groundwater radon contamination is a common occurrence in areas underlain by granite and by granite gneiss and other high grade metamorphic rocks. In a recent study by Dillon (1989), approximately 300 wells in the Athens region of Northeast Georgia were sampled and the groundwater tested for radon gas. The above area covers almost 9,000 square kilometers located to the east and southeast of Atlanta, Georgia. The area is situated in the Inner Piedmont belt and is underlain entirely by igneous and metamorphic rocks. The available measurements exhibit complex spatial variations which preclude error-free deterministic regional estimation and mapping of groundwater radon contamination. In view of this high degree of variation, a non-linear geostatistical tool, known as indicator kriging is employed to produce spatial risk maps of radon concentrations. The spatial extent of these high risk areas depend on three factors: (i) observed values; (ii) the desired risk level; and (iii) the pre-determined threshold (safe) value of contamination. Such maps will aid a geohydrologist to determine the areas with high risk of radon contamination and target them for more intensive monitoring, remedial, and/or regulatory actions. All computer works and mapping are conducted using GEO-EAS, which is a public domain microcomputer geostatistical environmental assessment software, developed by U.S. Environmental Protection Agency.

INTRODUCTION

Radon-222 (radon) is a naturally occurring, colorless, odorless, tasteless, inert, radioactive gas which is a product of the uranium-238 (U-238) decay series. Due to the omnipresence of uranium in the earth's rock and soils, radium and radon are found everywhere in our environment to some degree. Generally high concentrations of radon are known to exist in areas underlain by granite and by granite gneiss and other high grade metamorphic rocks. One of the major sources of and mechanism for radon migration is the groundwater. Radon can enter the home air through the degassing of water used for household activities such as dishwashing and showering. This has caused serious concerns, since radon has been associated with cancer of the lungs (bronchial epithelium) and tissue damage in stomach. Cross *et al.* (1985) suggest a safe limit of 10,000 pCi/l of radon in public drinking water.

In a recent study by Dillon (1989), approximately 300 wells in the Athens region of Northeast Georgia, U.S.A. were sampled and the groundwater was tested for radon gas. The above area covers almost 9,000 square kilometers located to the east and southeast of Atlanta, Georgia. The area is situated in the Inner Piedmont belt and is underlain entirely by igneous and metamorphic rocks. There are a number of different water-bearing units in this region. Preliminary studies by the above author indicate that geology of each water-bearing unit is the primary factor of radon occurrence in groundwater. Different lithologies appear to have varying radon production potentials which affect the radon levels in the water.

In this study, we focus our attention on observed values from water-bearing unit A, as defined by Radtke *et al.* (1986). This unit is composed of granite, granite-gneiss, and schist, which contains more observation wells than other units. There are 104 observation sites scattered over an area of about 8,000 square kilometer as shown in Figure 1. The observed values range from 154,767 pCi/l to 160 pCi/l with a median of 2355 pCi/l. The spatial distribution of these values are so complex that it warrants the use of the probability theory. In other words, the measured values are viewed as a realization of a spatial random function.

MAPPING METHOD

Many physical phenomena exhibit complex variations in space. In most instances, these spatial fluctuations are so complicated that they preclude the use of error-free deterministic predictions, even when data are available. Samples or measurements taken at different locations within the same hydrological system display a wide range of variability. As a consequence, one cannot predict with certainty the value of such a variable at an unmeasured

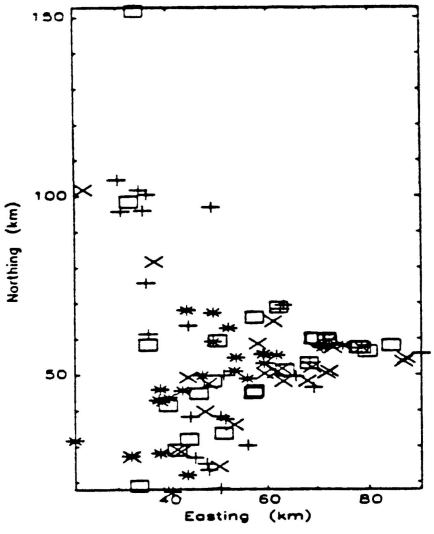

1st Quartile: 160.00≤ + ≤ 1330.000
2nd Quartile: 1330.00< x ≤ 2310.000
3rd Quartile: 2310.00< □ ≤ 5560.000
4th Quartile: 5560.00< * ≤ 1547 67.100

Figure 1. Measurement Locations of Radon-222, Water-Bearing Unit A< The Athens Region, Northeast Georgia, USA (Symbols indicate the observed value).

site, even if it has been measured at other nearby wells.

Geostatistics (Matheron, 1971; Journel and Huijbregts, 1978) recognizes these difficulties and provides the statistical tools for various estimation tasks. For an overview of geostatistical techniques and applications see ASCE (1990 a and 1990 b).

One of the geostatistical non-parametric estimation techniques is known as indicator kriging (Journel, 1984; Sullivan, 1984). This procedure provides estimates of conditional probabilities of the variable of interest. In indicator kriging the original measured values are transformed into indicator variables, such that they are zero if the datum values are less than the cut-off level, or unity if otherwise. So the indicator value, i_k, for a cut-off value z_k, at location x, is defined as:

$$i_k(x) = 1 \text{ if } z(x) \le z_k$$

or

$$i_k(x) = 0, \text{ otherwise} \qquad (1)$$

The interpolated indicator variable at any point, x_0, is then estimated by kriging, as follows

$$i_k^*(x_0) = \sum_{j=1}^{N} \lambda_{j0} i_k(xj) \qquad (2)$$

where, x_j, j = 1,...,N, represent the location of sampled points, and λ_{j0} is the kriging weight for the indicator value at point x_j in the estimation of i at point x_0. $i_k^*(x_0)$ is an estimate of the conditional probability at x_0, i.e., Prob[$z(x_0) \le z_k/z(x_j)$]. By varying the value of z_k, we can estimate the different i_k which allow us to construct the cumulative probability of Z^* at x_0.

To use indicator kriging, the semi-variogram of indicator values for each cut-off level must be determined. Using these different semi-variograms gives rise to the dependence of the kriged values on the cut-off level, which may lead to order-relation problem, where the estimated conditional probability decreases for increasing cut-off levels, has negative values, or values greater than unity. Kim (1984) offers some practical solutions to these order-relation problems.

Having the plot of cumulative distribution of Z^* at every estimated point, one can directly determine the risk values of Z_α at those sites without making any assumption concerning the distribution of Z^*. The risk values can then be mapped based on kriging techniques.

RADON RISK MAPS

In order to conduct indicator kriging, six cut-off values of 1,000., 2,355., 5,000., 10,000., 50,000., and 100,000. pCi/l are used. For each of these cut-off value a semi-variogram is estimated. Based on the above semi-variograms the indicator values are kriged over a section of the study area between 20 and 80 km North, and 20 and 80 km East. At every estimation grid, x, a cumulative distribution is constructed by plotting estimated $i_k^*(x)$ verses its corresponding cut-off value, z_k. Figure 2 depicts two samples of such cumulative distribution functions. As illustrated, each location may have a different distribution characteristics depending on the values of its neighboring points. From cumulative distribution functions one can determine different risk values of Z.

The risk value $Z_\alpha(x)$ is defined as such value whose probability of exceedence, i.e., Prob[$Z(x) < Z_\alpha(x)$] = 1 - α. As α decreases there will be a lower chance of exceeding Z_α, and consequently less risk. Having determined the Z_α for the appropriate risk level, α, at all grid points, we proceed to produce their contour maps. As an example, the 50% (median) and 10% risk maps of radon values are shown in Figure 3. The potentially hazardous areas, defined as those zones were $Z_\alpha \ge$ 10,000. pCi/l, are shown as shaded areas. The extent of these areas depend on the risk level, such that as α decreases from 50% to 10% the size of the hazardous areas decreases, too. So depending on the level of our preferred risk we can determine those areas where the groundwater users may encounter radon contamination.

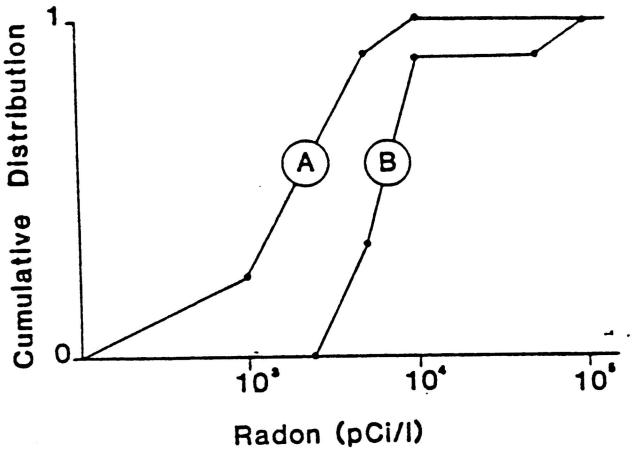

Figure 2. Cumulative Distribution at Point A (60,40), and at Point B (80,70). (Coordinates are given in kilometers).

CONCLUSIONS

The above work clearly demonstrates the usefulness of geostatistical techniques in analysis of natural phenomena in regional water resources studies. In particular, the non-parametric procedure of indicator kriging allows us to construct the probability distributions of our estimated values without any assumption about the underlying distribution of the variable of interest. This technique is most appropriate in cases where the observed data exhibit non-normal characteristics. This flexible method produces risk maps which may be used by decision makers to define the extent of hazardous areas based on various risk criteria.

It must be noted that all computer works and mappings are conducted using GEO-EAS, which is a public domain micro-computer geostatistical environmental assessment software, developed by U.S. Environmental Protection Agency (Englund and Sparks, 1988).

LITERATURE CITED

ASCE Task Committee on Geostatistical Techniques in Geohydrology (S. Rouhani, Chairman), "Review of Geostatistics in Geohydrology, 1. Basic Concepts," ASCE Journal of Hydraulic Engineering, 116(5), 612-632, 1990 a.

ASCE Task Committee on Geostatistical Techniques in Geohydrology (S. Rouhani, Chairman), "Review of Geostatistics in Geohydrology, 2. Applications," ASCE Journal of Hydraulic Engineering, 116(5), 633-658, 1990 b.

Cross, F.T., H.H. Harley, and W. Hofmann, "Health Effects and Risks from Rn-222 in Drinking Water," Health Physics, Vol. 48, p. 649, 1985.

Dillon, M.E., "A Study of Radon-222 in Groundwater in the Athens Region of Northeast Georgia: Concentration as a Function of the Geologic and Hydrogeologic Conditions," M.S. Thesis, School of Geophysical Sciences, Georgia Institute of Technology, Atlanta, 1989.

Englund, E., and A. Sparks, "GEO-EAS (Geostatistical Environmental Assessment Software) User's Guide," EPA600/4-88/033, EMSL, EPA, Las Vegas, 1988.

Journel, A.G., "The Place of Non-Parametric Geostatistics," in G. Verly et al., Editors, Geostatistics for Natural Resources Characterization, Part I, D. Reidel Publishing Co., Dordrecht, 307-335, 1984.

Journel, A.G., and C.J. Huijbregts, Mining Geostatistics, Academic Press, London, 600 p., 1978.

Kim, Y.C., "Lecture Notes on Indicator and Probability Kriging," University of Arizona, Tuscon, 1984.

Matheron, G., The Theory of Regionalized Variables and Its Applications, Les Cahiers du Centre de Morphologie Mathématique de Fontainebleau, No. 5, 211 p., 1971.

Radtke, D.B., W.C. Cressler, H.A. Perlman, H.E. Blanchard, K.W. McFadden, and R. Brooks, "Occurrence and Availability of Ground Water in The Athens Region, Northeast Georgia," U.S.G.S. Water Resources Investigation Report 86-4075, 79 p., 1986.

Figure 1. Measurement Locations of Radon-222, Water- Bearing Unit A, The Athens Region, Northeast Georgia, USA (Symbols indicate the observed value).

Distribution at Point A (60, 40), and at Point B (80,70). (Coordinates are given in kilometers).

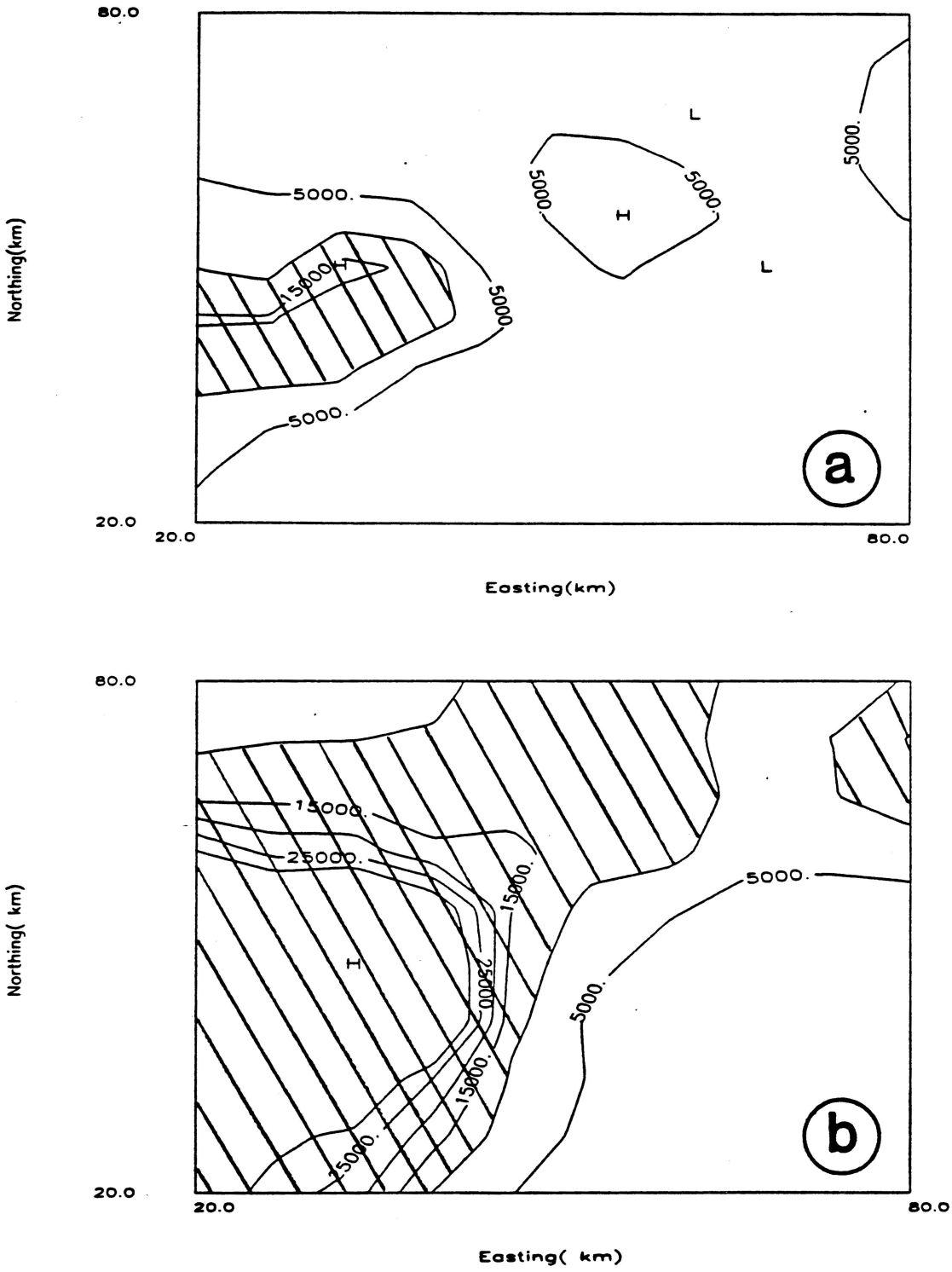

Figure 3. (a) 50% Radon Risk Map, and (b) 10% Radon Risk Map. (Shaded areas correspond to those locations where $Z_\alpha \geq 10{,}000.$ pCi/l).